Stem Cell Reports
Report
ISSCR
OPEN ACCESS

The aPKC-CBP Pathway Regulates Post-stroke Neurovascular Remodeling and Functional Recovery

Ayden Gouveia,[1,2] Matthew Seegobin,[1] Timal S. Kannangara,[2,9] Ling He,[3] Fredric Wondisford,[4] Cesar H. Comin,[5] Luciano da F. Costa,[6] Jean-Claude Béïque,[2,7,8,9] Diane C. Lagace,[2,7,8,9] Baptiste Lacoste,[2,7,8,9] and Jing Wang[1,2,7,9,*]

[1]Regenerative Medicine Program, Ottawa Hospital Research Institute, Ottawa, ON K1H 8L6, Canada
[2]Department of Cellular and Molecular Medicine, Faculty of Medicine, University of Ottawa, Ottawa, ON, Canada
[3]Department of Pediatrics and Medicine, Johns Hopkins Medical School, Baltimore, MD, USA
[4]Department of Medicine, Rutgers-Robert Wood Johnson Medical School, New Brunswick, NJ, USA
[5]Department of Computer Science, Federal University of São Carlos, São Carlos, São Paulo, Brazil
[6]São Carlos Institute of Physics, University of São Paulo, PO Box 369, São Carlos, São Paulo 13560-970, Brazil
[7]University of Ottawa Brain and Mind Research Institute, Ottawa, ON, Canada
[8]Neuroscience Program, Ottawa Hospital Research Institute, Ottawa, ON, Canada
[9]Canadian Partnership for Stroke Recovery, Ottawa, ON, Canada
*Correspondence: jiwang@ohri.ca
https://doi.org/10.1016/j.stemcr.2017.10.021

SUMMARY

Epigenetic modifications have emerged as attractive molecular substrates that integrate extrinsic changes into the determination of cell identity. Since stroke-related brain damage releases micro-environmental cues, we examined the role of a signaling-induced epigenetic pathway, an atypical protein kinase C (aPKC)-mediated phosphorylation of CREB-binding protein (CBP), in post-stroke neurovascular remodeling. Using a knockin mouse strain (*Cbp*S436A) where the aPKC-CBP pathway was defective, we show that disruption of the aPKC-CBP pathway in a murine focal ischemic stroke model increases the reprogramming efficiency of ischemia-activated pericytes (i-pericytes) to neural precursors. As a consequence of enhanced cellular reprogramming, *Cbp*S436A mice show an increased transient population of locally derived neural precursors after stroke, while displaying a reduced number of i-pericytes, impaired vascular remodeling, and perturbed motor recovery during the chronic phase of stroke. Together, this study elucidates the role of the aPKC-CBP pathway in modulating neurovascular remodeling and functional recovery following focal ischemic stroke.

INTRODUCTION

Stroke is a major public health burden with 40% of patients suffering from permanent neurological disabilities, and novel post-stroke interventions are urgently needed (Krueger et al., 2015). Increasing evidence shows that multipotent neural precursors (NPCs) in the injury site not only migrate from the lateral ventricle subventricular zone (SVZ) in adult brain (Jin et al., 2003; Dibajnia and Morshead, 2013) but are also reprogrammed from local non-neuronal cells following stroke (Shimada et al., 2012; Nakagomi et al., 2015). Pericytes that wrap endothelial cells in the capillaries have emerged as an attractive cell resource, which can be reprogrammed to tissue-specific stem cells following injury (Dellavalle et al., 2011; Tatebayashi et al., 2017). In stroke-related brain injury, a mesenchymal-epithelial transition process is involved in cellular reprogramming of pericytes to multipotent NPCs (Nakagomi et al., 2015). In addition to its plasticity in cellular reprogramming, pericytes are also important for the vascular remodeling post stroke by stabilizing the newly generated microvessel walls and maintaining the blood brain barrier (Liu et al., 2012; Armulik et al., 2010).

We recently identified a signaling-directed epigenetic pathway, atypical protein kinase C (aPKC)-mediated S436 phosphorylation in CREB-binding protein (CBP), and its roles in regulating neuronal differentiation of NPCs in both the developing and aging brain, where marked changes in cell-extrinsic signals occur (Wang et al., 2010; Gouveia et al., 2016). Since stroke-related brain injury releases a plethora of cytokines and inflammatory and growth factors (Kalluri and Dempsey, 2008; Doll et al., 2014), such a pool of enriched extrinsic signals, resembling what occurs in the developing or aging brain, may act on the aPKC-CBP pathway to modulate cell fate, including cellular reprogramming and differentiation. Since CBP is a key epigenetic switch to regulate the epithelial-mesenchymal transition process (Abell et al., 2011), it is intriguing to examine the role of the aPKC-CBP pathway following stroke in regulating NPC reprogramming from pericytes.

Here, we identify a transient population of locally derived NPCs that are reprogrammed from pericytes in the injury site shortly after stroke. The permanent deletion of the aPKC-CBP pathway enhances the pericyte reprogramming efficiency to multipotent NPCs, consequently exhausting proliferative pericytes and compromising vascular remodeling to impair post-stroke functional recovery. Here, we show that reactivation of the aPKC-CBP pathway is required for stroke functional recovery in the chronic phase through neurovascular remodeling.

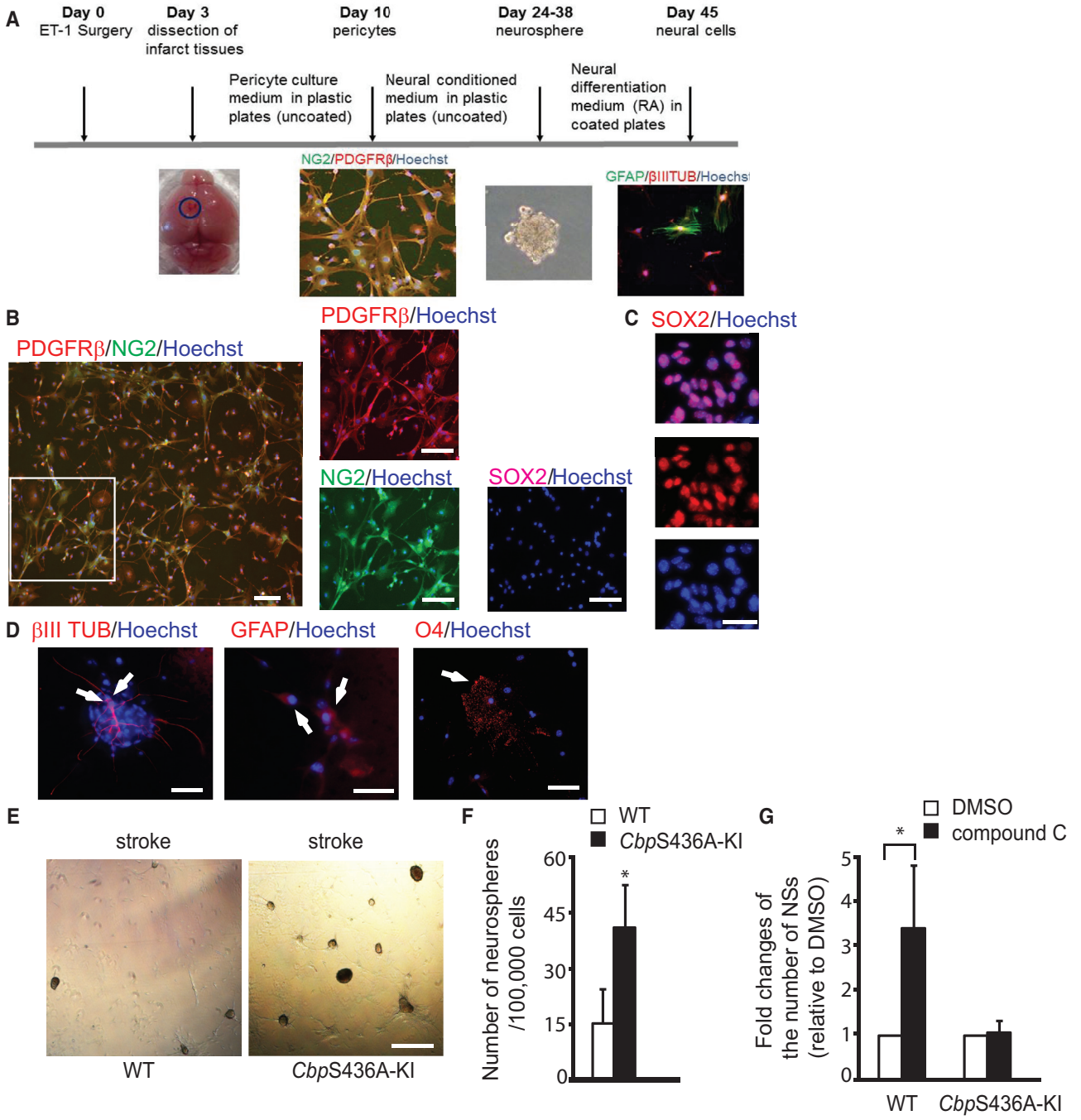

Figure 1. *Cbp*S436A Enhances the Reprogramming Efficiency of i-Pericytes to NPCs in Culture

(A) Schematic of experimental flowchart.

(B) Images of i-pericytes cultured for 7 days, showing PDGFRβ+ (red)/NG2+ (green)/SOX2− (purple) cells. Scale bar, 25 μm.

(C) A neurosphere reprogrammed from i-pericytes expressed Sox2 (red) after cytospin. Scale bar, 10 μm.

(D) Differentiation of neurospheres that were reprogrammed from i-pericytes into βIII TUBULIN+ neurons (left panel), GFAP+ astrocytes (middle panel), and O4+ oligodendrocytes (right panel) in the presence of retinoic acid. Arrows denote positive cells for βIII TUBULIN, GFAP, or O4. Scale bar, 20 μm.

(legend continued on next page)

RESULTS

Disruption of the aPKC-CBP Pathway Increases NPC Reprogramming from i-Pericytes in Culture

We used endothelin-1 (ET-1)/L-NAME stereotaxic co-injections to induce focal ischemic stroke in the sensorimotor cortex and examined the reprogramming capability of ischemia-activated pericytes (i-pericytes) to SOX2+ NPCs. To test this, we dissected the peri-infarct/infarct cortex tissues 3 days after ET-1/L-NAME injections and selectively isolated pericytes (PDGFRβ+/NG2+/SOX2−) by culturing single dissociated cells on an uncoated plastic culture dish. These i-pericytes were reprogrammed into NPCs in culture by forming neurospheres expressing SOX2 (Figures 1A–1C and S1). These i-neurospheres reprogrammed from i-pericytes were able to further differentiate into neurons, astrocytes, and oligodendrocytes (Figure 1D). Interestingly, i-pericytes from *Cbp*S436A-KI mice produced a greater number of neurospheres (Figures 1E and 1F). In addition, compound C, an AMPK inhibitor, showed the same potency to increase the number of neurospheres that were reprogrammed from wild-type (WT) i-pericytes (Figure 1G), while having no effect on *Cbp*S436A-KI i-pericytes. Together, these data suggest that disruption of the aPKC-CBP pathway improves the reprogramming efficiency of i-pericytes to NPCs.

Disruption of the aPKC-CBP Pathway Increases the Transient Population of Locally Derived NPCs that Are Reprogrammed from i-Pericytes in the Post-stroke Brain

To ask whether i-pericytes can be reprogrammed to NPCs *in vivo*, we investigated the locally derived NPCs in our focal ischemic stroke model. To first confirm if the SOX2+ NPCs in post-stroke cortex layer I were locally derived and did not migrate from the SVZ, we used a *Nestin*$Cre\text{-}ER^{T2}/tdTomato^{flx/Stop/flx}$ reporter line to trace SVZ NPCs by injecting tamoxifen 7 days before stroke surgery (Figure 2A). We found that tdTomato (TDT)+ cells in the SVZ were co-labeled with SOX2, and the TDT+SVZ NPCs did not migrate up to layer I at 7 days after stroke (Figure 2A). In addition, SOX2+NPCs in post-stroke cortex layer I were negative for TDT (Figure 2B). Next, to test whether the SOX2+NPCs in layer I were derived from pericytes following stroke, we performed an *in vivo* labeling experiment using the NeuroTrace 500/525 technology to label capillary pericytes in the live brain (Damisah et al., 2017). NeuroTrace 500/525 (300 nL) was injected intracortically just below the pia surface before ET-1/L-NAME injections. Three days post stroke, NeuroTrace-labeled pericytes were imaged *ex vivo* in the stroke-injured live cortical sections using two-photon microscopy. Sequentially, the same injured cortical sections were fixed and immunostained for SOX2 and imaged using confocal microscopy. Using the needle track landmarks to merge the two images, we were able to detect NeuroTrace+/SOX2+ cells, suggesting the pericyte origin of these SOX2+NPCs (Figure S2A). Third, we injected 5-bromo-2′-deoxyuridine (BrdU) 24 hr before surgery (Figure S2B) and sacrificed mice 3 days post-stroke. SOX2+NPCs in the injured cortex were negative for BrdU (Figure S2B), suggesting that they were derived from non-cycling cells pre-stroke. In addition, we used a *Sox2-GFP* reporter line, together with ethynyl 2′ deoxyuridine (EdU) post-stroke injections (Figure S2C), to show that *Sox2*-GFP+NPCs presented in both the SVZ and injured cortex layer I, co-labeling with EdU that marked proliferating cells. Together, these data suggest that SOX2+NPCs in injured cortex layer I were locally derived following stroke, possibly from capillary pericytes. Since SOX2+ cells from injured cortex were also NESTIN+ (detected either by a *Nestin-GFP* reporter line or Nestin-antibody) and adjacent to CD31+ microvessels (Figures 2C, 2D, and S2D), we further examined the identity of the specific population of NESTIN+ cells that were adjacent to microvessels and found that these NESTIN+ cells were co-labeled with two pericyte markers, PDGFRβ and NG2 (Figure 2E). These data further confirmed that the locally derived SOX2+NPCs in the injured cortex are reprogrammed from pericytes following stroke. We then assessed dynamic changes of NESTIN+/SOX2+ NPCs that were adjacent to microvessels at 3, 7, and 14 days post stroke in injured cortex layer I and observed that the locally derived NESTIN+/SOX2+ cells peaked 3 days post stroke and gradually diminished 14 days post stroke (Figures 2F, 2G, and S2E). Interestingly, another population of dorsal committed NPCs expressing both PAX6 and NESTIN surged to peak 7 days post stroke, followed by a rise of DCX+ neuroblasts 14 days post stroke in the same infarct region (Figures 2F and 2G). The sequential wave of three populations of cells in cortex layer I infarct implies a developmental process of locally derived NPCs that were reprogrammed from pericytes following stroke.

(E and F) Images (E) and quantitative analysis (F) of the number of neurospheres reprogrammed from i-pericytes isolated from wild-type (WT) and *Cbp*S436A-KI stroke tissues. Scale bar, 150 μm. *$p \leq 0.05$, n = 4/group.

(G) Quantitative analysis of the number of neurospheres reprogrammed from i-pericytes in the absence and presence of compound C (1 μM). *$p \leq 0.05$, n = 4/group.

Error bars in this figure represent the SEM.

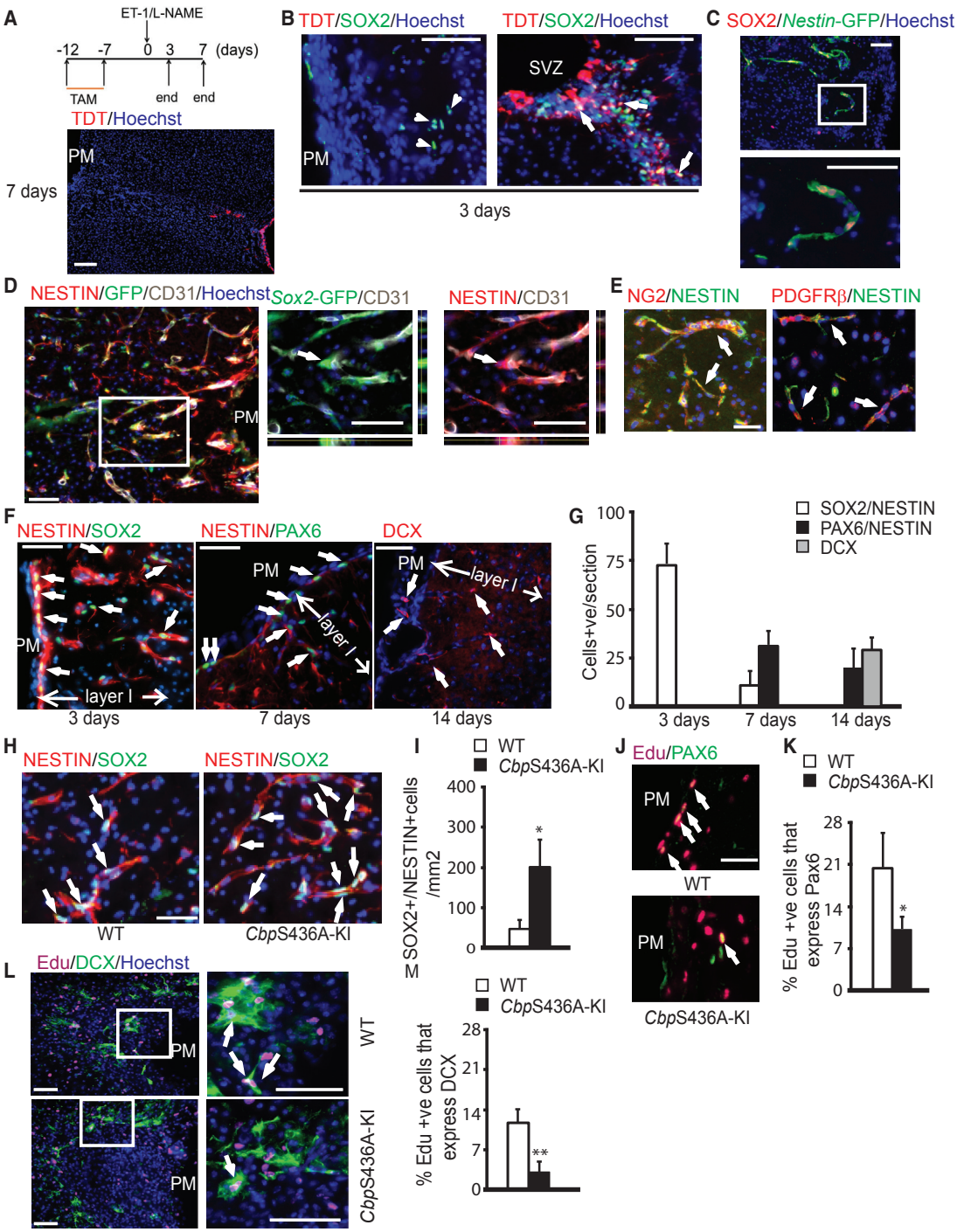

Figure 2. *Cbp*S436A Increases the Transient Population of Locally Derived NPCs that Are Reprogrammed from Pericytes in the Post-stroke Brain

(A and B) Expression of SOX2+ (green)/TDT+ (red) NPCs in the SVZ of *NestinCre-ER*^{T2}/*tdTomato*$^{flx/Stop/flx}$ mice, receiving tamoxifen before stroke, at 3 days (B) and 7 days (A) post stroke, while SOX2+NPCs in injured cortex layer I were negative for TDT 3 days post stroke. Arrows denote co-labeled cells, while arrowheads denote single-labeled cells with SOX2+. Scale bar, 100 μm (A); 40 μm (B). PM, pia mater; LV, lateral ventricle; TDT, TdTomato.

(C) Expression of GFP+ (green) and SOX2+ (red) cells in injured cortex of *Nestin*-GFP mice 3 days post stroke. White boxed image is enlarged in the bottom panel. Scale bar, 25 μm.

(legend continued on next page)

After identifying the transient population of locally derived NPCs, we further examined their developmental process in *Cbp*S436A-KI mice. The quantification analysis revealed that *Cbp*S436A-KI mice displayed an increase in the population of NESTIN+/SOX2+ NPCs 3 days post stroke (Figures 2H and 2I), while showing a reduced number of PAX6+ dorsal committed NPCs (Figure S2F) and DCX+ neuroblasts (Figure S2F) in layer I of the infarct cortex. We further used EdU pulse labeling post stroke (2–5 days post stroke) and showed that the proportion of PAX6+ dorsal committed NPCs (Figures 2J and 2K) and the proportion of DCX+ neuroblasts (Figures 2L and 2M) over total EdU+ cells were decreased in *Cbp*S436A-KI mice 14 days post stroke.

The aPKC-CBP Pathway Regulates Post-stroke Vascular Remodeling

To further confirm that the increased SOX2+/NESTIN+ NPCs in *Cbp*S436A-KI mice indeed originate from increased reprogramming of i-pericytes, we showed that the proportion of PDGFRβ+ pericytes over total EdU+ cells was decreased in *Cbp*S436A-KI mice (Figures 3A and 3B). The effect occurred independently of any difference between WT and *Cbp*S436A-KI in terms of basal number of pericytes under physiological conditions (Figures S3A and S3B) and the number of apoptotic i-pericytes following stroke (Figure S3C). These data suggest that the pool of proliferative i-pericytes exhausted over time due to increased reprogramming. Since pericytes are known to stabilize newly formed blood vessels and neurovascular units (Daneman et al., 2010; Sweeney et al., 2016), we further determined whether post-stroke vascular remodeling and angiogenesis were hampered by the increased reprogramming process. To assess vascular remodeling post stroke, brain sections collected at 14 days post stroke from both genotypes were immunostained for CD31 to label endothelial cells. The density of CD31+ microvessels and the area of vascular coverage were reduced in the ipsilateral cortex from both genotypes (Figures 3C–3E) relative to contralateral. Importantly, *Cbp*S436A-KI mice showed a significant decrease in the number of CD31+ microvessels and vascular coverage when compared with WT mice in the ipsilateral cortex (Figures 3C–3E). In addition, we performed three-dimensional (3D) cortical vasculature analysis using brains collected at 25 days post stroke (Figures 3F–3H). Ipsilateral vessel length and branchpoints from WT mice showed a trend of being higher than those in the contralateral WT cortex, implying a sign of vascular remodeling. However, *Cbp*S436A-KI mice displayed a consistent reduction in the ipsilateral vessel length and branchpoints when compared with their contralateral count and with those from WT mice (Figures 3F–3H). To assess post-stroke angiogenesis, we performed EdU pulse labeling as previously described and examined brain sections 14 days after stroke by immunohistochemistry. The percentage of EdU+/CD31+ newly generated blood vessels was significantly reduced in *Cbp*S436A-KI mice (Figures 3I and 3J). Thus, disruption of the aPKC-CBP pathway increases cellular reprogramming of i-pericytes at the expense of vascular remodeling post stroke.

The aPKC-CBP Pathway Modulates Post-stroke Functional Recovery without Altering Stroke Volume

To assess outcomes of the altered neurovascular remodeling in *Cbp*S436A-KI mice, we examined stroke volume and performed behavioral analysis. There was no significant difference in infarct volume between WT and *Cbp*S436A-KI mice at 3 and 14 days post stroke (Figures 4A and 4B). To assess post-stroke functional recovery, both genotypes of mice were tested on two sensitive behavioral tests that measure motor deficits: the horizontal ladder run and cylinder tasks. On the horizontal ladder task, WT and *Cbp*S436A-KI mice showed a comparable baseline pre-stroke and a similar increase in step error 7 days post stroke in both the contralateral and ipsilateral forelimbs (Figure 4C). By 14 days post stroke, *Cbp*S436A-KI mice had significantly more deficits compared with

(D) Expression of GFP+ (green)/NESTIN+ (red) co-labeled NPCs that were adjacent to CD31+ (white) endothelial cells in injured cortex of *Sox2*-GFP mice 3 days post stroke. White boxed image is enlarged in the right panels. Arrows denote co-labeled GFP+/NESTIN+ cells. Scale bar, 25 μm.

(E) NESTIN+ cells within the infarct core are co-labeled with other pericyte markers, NG2 (red, left panel) and PDGFRβ (red, right panel). Arrows denote co-labeled cells. Scale bar, 20 μm.

(F and G) Images (F) and quantification (G) of SOX2 (green)/NESTIN+ (red, left panel) NPCs, PAX6 (green)/NESTIN+ (red, middle panel) NPCs and DCX+ (red, right panel) neuroblasts in injured cortex layer I 3, 7, and 14 days post stroke. Arrows represent positive cells that were quantified for (G). Scale bar, 20 μm.

(H and I) Images (H) and quantification (I) of co-labeled SOX2+/NESTIN+ NPCs in WT and *Cbp*S436A ipsilateral cortex 3 days post stroke. Arrows denote co-labeled cells. Scale bar, 20 μm. *$p < 0.05$, n = 3–4/group.

(J–M) Images (J and L) and quantification (K and M) of co-labeled PAX6+/EdU+ NPCs (J and K) and DCX+/EdU+ neuroblasts (L and M) in WT and *Cbp*S436A ipsilateral cortex 14 days post stroke, injected with EdU days 2–5 post stroke. White boxed image is enlarged in the right panels. Arrows denote co-labeled cells. Scale bar, 25 μm. *$p < 0.05$; **$p < 0.01$, n = 3–4/group.

Error bars in this figure represent the SEM.

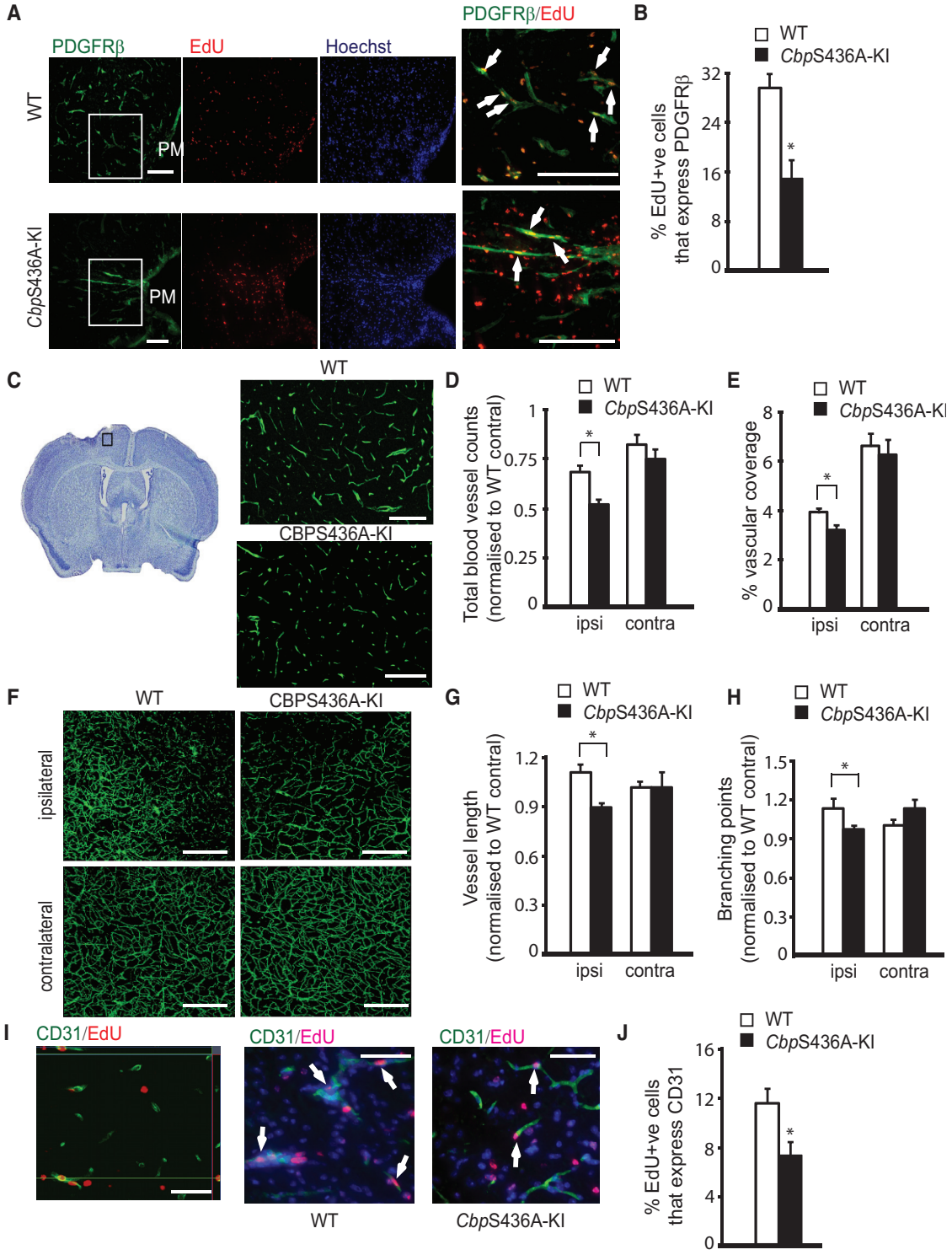

Figure 3. *Cbp*S436A regulates Post-stroke Vascular Remodeling

(A and B) Images (A) and quantification (B) of co-labeled PDGFRβ+/EdU+ pericytes in WT and *Cbp*S436A ipsilateral cortex 14 days post stroke. Arrows denote co-labeled cells. Scale bar, 50 μm. *$p < 0.05$, n = 3/group.

(C) Images of CD31 (green) in injured cortex from WT and *Cbp*S436A mice 14 days post stroke (right panel). Scale bar, 100 μm.

(legend continued on next page)

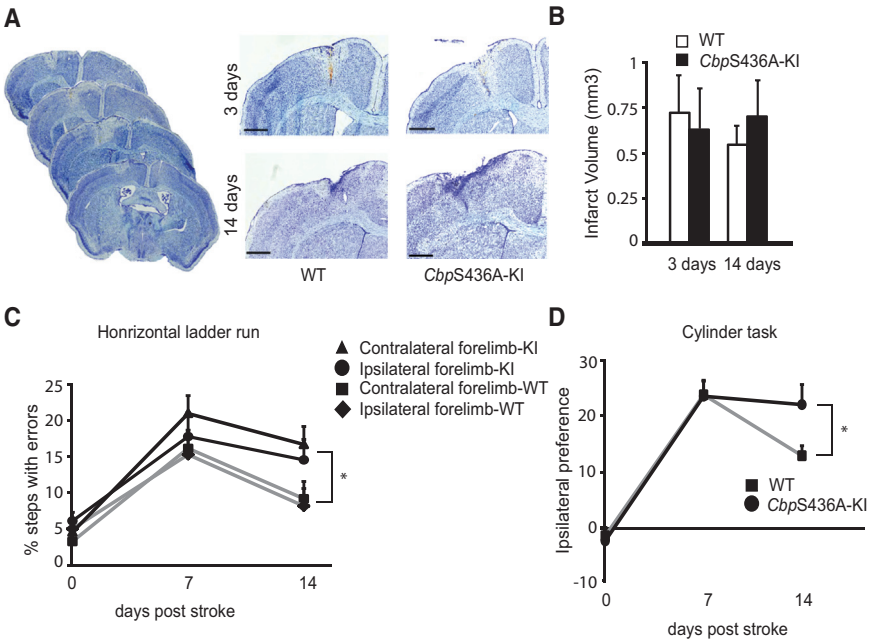

Figure 4. *Cbp*S436A Modulates Post-stroke Functional Recovery without Altering Stroke Volume

(A and B) Images (A) and quantification (B) of infarct volumes at 3 and 14 days post stroke from WT and *Cbp*S436A-KI mice. Scale bars, 50 μm (n = 6/group for 3 days; n = 9/group for 14 days).

(C) The percentage of forelimb error step at 7 and 14 days post stroke in WT and *Cbp*S436A mice, analyzed by two-way ANOVA (Time × Genotype with forelimbs $F(6,168) = 0.76$, $p = 0.7587$, n = 17 for WT, n = 13 for KI), with Tukey's post hoc test, *$p < 0.05$ compared with WT, n = 13–17/group.

(D) The ipsilateral preference in the cylinder test at 7 and 14 days post stroke in WT and *Cbp*S436A-KI mice, analyzed by two-way ANOVA (Time × Genotype $F(2,42) = 2.395$, $p = 0.1035$, n = 17 for WT, n = 13 for KI) with Tukey's post hoc test, *$p < 0.05$ compared with WT, n = 13–17/group.

Error bars in this figure represent the SEM.

WT mice on both limbs. A very similar pattern was shown in the cylinder test. Both WT and *Cbp*S436A-KI mice displayed no preference in using forepaws to touch the cylinder wall pre-stroke and a similar preference to use the ipsilateral forepaw 7 days post stroke (Figure 4D), while at 14 days post stroke *Cbp*S436A-KI mice had a significantly higher ipsilateral preference, implicating less recovery in *Cbp*S436A-KI mice. Thus, the aPKC-CBP pathway modulates post-stroke functional recovery without altering stroke volume.

DISCUSSION

The current study identifies a transient population of locally derived NPCs following focal ischemic stroke, reprogrammed from i-pericytes. We further demonstrate that phosphomutant *CbpS436A* enhances the reprogramming efficiency of i-pericytes to NPCs both in culture and *in vivo*. As a consequence, permanent deletion of the aPKC-CBP pathway reduces the population of proliferating pericytes following stroke, leading to perturbed vascular remodeling and stroke motor functional recovery deficits.

Increasing evidence suggested that pericytes have the capability to be reprogrammed into multipotent NPCs or mature neurons both *in vitro* and *in vivo* (Nakagomi et al., 2015; Tatebayashi et al., 2017; Karow et al., 2012). Here, we demonstrate that i-pericytes following focal ischemic stroke can be reprogrammed to SOX2+NPCs, transiently arising shortly after stroke (3 days) followed by another wave of PAX6+ dorsal committed NPCs peaking 7 days after stroke. More importantly, we found that a single S436 phosphorylation mutation in CBP significantly increases the reprogramming efficiency of i-pericytes to SOX2+ NPCs, while arresting the reprogrammed NPCs at the early

(D and E) Quantification of total blood vessel counts (D) and the percentage of vascular coverage (E) from ipsilateral and contralateral cortex of WT and *Cbp*S436A mice as shown in (C), normalized to the average counts of the WT contralateral group. Data were analyzed by two-way ANOVA(Genotype × Hemisphere interaction $F(1,24) = 1.116$, $p = 0.3022$, Genotype $F(1,24) = 18.52$, $p = 0.0003$, n = 7/per group for total blood vessel counts; Genotype × Hemisphere interaction $F(1,12) = 0.225$, $p = 0.649$, Genotype $F(1,12) = 0.58$ $p = 0.0001$, n = 4/per group for vascular coverage), with Tukey's post hoc test, *$p < 0.05$, n = 4–7/group.

(F) Confocal images of cortex of WT and *Cbp*S436A mice 25 days post stroke, stained for CD31 (green). Scale bar, 100 μm.

(G and H) Quantitative analysis of vessel length (G) and branchpoints (H), normalized as fold change over contralateral (Genotype × Hemisphere interaction $F(1,12) = 4.317$, $p = 0.3022$ for vessel length; Genotype × Hemisphere interaction $F(1,12) = 5.372$, $p = 0.0389$ for branchpoints) (n = 5 for WT, n = 3 for KI), with Tukey's post hoc test, *$p < 0.05$, n = 3–5/group.

(I and J) Images (I) and quantification (J) of co-labeled CD31+/EdU+ endothelial cells in WT and *Cbp*S436A ipsilateral cortex 14 days post stroke. Arrows denote co-labeled cells. Scale bar, 20 μm. *$p < 0.05$, n = 3/group.

Error bars in this figure represent the SEM.

stage without progressing into PAX6+ dorsal committed NPCs. This is a very interesting observation. Previously, we showed that *Cbp*S436A led to differentiation deficits in the hippocampal subgranular zone (SGZ) SOX2+NPCs, arrested at an early stage without progressing to mature neurons (Gouveia et al., 2016). This suggests that *Cbp*S436A has two roles in regulating NPC reprogramming and differentiation: facilitating NPC reprogramming from i-pericytes while simultaneously preventing their further differentiation. Another possible explanation for the reduction of PAX6+ dorsal committed NPCs is due to fate changes of SOX2+ multipotent stem cells. SOX2 is not only considered as a marker for neural precursors but also as a marker for pluripotency. A previous study has shown that pluripotent-like stem cells were detected in the injured cortex following transient middle cerebral artery occlusion, labeled with pluripotent markers, SOX2, KL4, and c-MYC (Nakagomi et al., 2015). In addition, IBA1+ microglia have been shown to be reprogrammed from i-pericytes (Sakuma et al., 2016). To assess the possibility that the reduced number of PAX6+ cells in *Cbp*S436A-KI is due to an increased number of Iba1+ microglia, possibly generated from SOX2+ pluripotent/multipotent stem cells, we examined the proportion of IBA1+ microglia in the total EdU+ cells 14 days post stroke. Indeed, the proportion of IBA1+ microglia was increased in *Cbp*S436A-KI compared with their WT littermates (Figures S3D and S3E). These findings suggest that there could be a change in fate between PAX6+ NPCs and IBA1+ microglial cells, which remains to be confirmed in future studies utilizing lineage tracing experiments.

Histone acetyltransferases such as CBP are well known to regulate cell-fate changes (Krishnakumar and Blelloch, 2013; Murao et al., 2016). Increasing studies have targeted either bromodomain or histone deacetylase activity to increase the reprogramming efficiency of nonneruonal cells to NPCs and mature neurons (Li et al., 2015; Pfisterer et al., 2016; Gao et al., 2017). Despite this, a direct signal that modulates histone acetyltransferase (HAT) activity to alter cell fate remains largely unknown. We previously showed that the aPKC-CBP pathway can be activated by metformin to enhance the neuronal differentiation of NPCs (Wang et al., 2012). Our current finding, instead, revealed that inactivation of the aPKC-CBP pathway enhances NPC reprogramming from i-pericytes. Thus, the aPKC-mediated single phosphorylation of CBP serves as a signaling sensor to fine-tune cell-fate decisions through reprogramming or differentiation processes. This phosphorylation in CBP may directly alter either the histone acetyltransferase activities or their chromatin-binding profiles. Identification of downstream targets of the aPKC-CBP pathway at both genomic and epigenomic levels will be further explored.

EXPERIMENTAL PROCEDURES

Animals

All animal use was approved by the Animal Care Committees of the University of Ottawa in accordance with the Canadian Council of Animal Care policies. Transgenic mouse lines, *Cbp*S436A, *Sox2-GFP*, *Nestin-GFP*, and *Nestin*Cre-ER^{T2}/tdTomato$^{flx/Stop/flx}$ mice were maintained on a 12 hr light/12 hr dark cycle with access to food and water *ad libitum*.

Detailed information is described in Supplemental Experimental Procedures.

ET-1/L-NAME Surgery

Mice (2–4 months) were anesthetized using 4%–5% isoflurane and 1.5% oxygen and mounted on a stereotaxic frame for ET-1/L-NAME injections, detailed in Supplemental Experimental Procedures.

Pericyte Culture and Sphere Formation

Three days following ET-1 surgery, mice were killed and their brains were dissected out. Pericyte culture isolated from injured cortex is detailed in Supplemental Experimental Procedures.

Drug Treatment

To label dividing cells or SVZ NPCs, mice received an intraperitoneal injection (i.p.) with EdU, BrdU, or tamoxifen, detailed in Supplemental Experimental Procedures.

Immunohistochemistry, Microscopy, and Quantification

Immunostaining of brain sections was performed as described previously (Gouveia et al., 2016), detailed in Supplemental Experimental Procedures. Detailed image acquisition and quantification is also described in Supplemental Experimental Procedures.

EdU Click-iT Chemistry Labeling

EdU was visualized using Click-iT chemical reaction kits from Cell Signaling (C10338) according to the manufacturer's instructions.

Three-Dimensional Blood Vessel Staining, Imaging, and Quantification

Mice were killed at 25 days post surgery, and the cortices were dissected, flattened between two layers of glass, and immersed in 4% paraformaldehyde overnight at 4°C. The detailed procedure is described in Supplemental Experimental Procedures.

Two-Photon *Ex Vivo* Imaging

Coronal slices were generated as described previously. Detailed imaging procedures are described in Supplemental Experimental Procedures.

Horizontal Ladder Test and Cylinder Test

The two tests were performed at the Behavioral Core at the University of Ottawa, detailed in Supplemental Experimental Procedures.

Cresyl Violet Staining and Infarct Volume Measurement

Slides containing serially collected sections were dried at 37°C for 15 min and stained with cresyl violet solution (Sigma-Aldrich, C5402), detailed in Supplemental Experimental Procedures.

Statistical Analysis

Data analysis was performed using GraphPad Prism 6 (Graphpad Software, La Jolla, CA). Behavioral analysis was performed using two-way ANOVA with Tukey's post hoc test. Single comparisons were performed using two-tailed Student's t test. n in the figure legends refers to individual mice.

SUPPLEMENTAL INFORMATION

Supplemental Information includes Supplemental Experimental Procedures and three figures and can be found with this article online at https://doi.org/10.1016/j.stemcr.2017.10.021.

AUTHOR CONTRIBUTIONS

A.G. performed stroke surgery, behavioral analysis, immunostaining, and pericyte culture; M.S. maintained the mouse colony; L.H. and F.W. generated the *Cbp*S436A knockin mouse strain. B.L., C.H.C., and L.d.F.C. designed and performed 3D vasculature assessments; D.C.L. designed and provided mice for the NestinCreER2 reporter mice experiments. J.-C.B., D.C.L., and T.S.K. designed and performed two-photon imaging on live brain sections. A.G. and J.W. contributed to experimental design, data interpretation, and writing the paper.

ACKNOWLEDGMENTS

This work was supported by J.P. Bickell Foundation, Ottawa Hospital Foundation and the Heart and Stroke Foundation (HSF) through a grant-in-aid (GIA-16-00014650) to J.W.; CNPq (307333/2013-2) and FAPESP (11/50761-2) grants to L.d.F.C.; FAPESP (15/18942-8) grant to C.H.C.; HSF Canadian Partnership for Stroke Recovery (CPSR) Trainee Award to T.S.K.; HSF CPSR and CIHR grants (MOP378718) to D.C.L.; and HSF CPSR, CIHR (MOP142420), and CFI (23915) grants to J.-C.B. We thank Anthony Carter (HSF CPSR) for ET-1 stroke surgery training, Dr. Hsiao-Huei Chen for a gift of anti-IBA1 and Dr. Ruth Slack for a gift of Sox2-GFP reporter mice. We also thank the uOttawa's Core facility program (CBIA) for infrastructure support.

Received: June 5, 2017
Revised: October 25, 2017
Accepted: October 26, 2017
Published: November 22, 2017

REFERENCES

Abell, A.N., Jordan, N.V., Huang, W., Prat, A., Midland, A.A., Johnson, N.L., Granger, D.A., Mieczkowski, P.A., Perou, C.M., Gomez, S.M., et al. (2011). MAP3K4/CBP-regulated H2B acetylation controls epithelial-mesenchymal transition in trophoblast stem cells. Cell Stem Cell. *8*, 525–537.

Armulik, A., Genove, G., Mae, M., Nisancigglu, M.H., Wallgard, E., Niaudet, C., He, L., Norlin, J., Linblom, P., Strittmatter, K., et al. (2010). Pericytes regulate the blood-brain barrier. Nature *25*, 557–561.

Damisah, E.C., Hill, R.A., Tong, L., Murray, K.N., and Grutzendler, J. (2017). A fluoro-Nissl dye identifies pericytes as distinct vascular mural cells during *in vivo* brain imaging. Nat. Neurosci. *20*, 1023–1032.

Daneman, R., Zhou, L., Kebede, A.A., and Barres, B.A. (2010). Pericytes are required for blood-brain barrier integrity during embryogenesis. Nature *468*, 562–566.

Dellavalle, A., Maroli, G., Covarello, D., Azzoni, E., Innocenzi, A., Perani, L., Antonini, S., Sambasivan, R., Brunelli, S., Tajbakhsh, S., and Cossu, G. (2011). Pericytes resident in postnatal skeletal muscle differentiate into muscle fibres and generate satellite cells. Nat. Commun. *2*, 499.

Dibajnia, P., and Morshead, C. (2013). Role of neural precursor cells in promoting repair following stroke. Acta Pharmacol. Sin. *34*, 78–90.

Doll, D.N., Barr, T.L., and Simpkins, J.W. (2014). Cytokines: their role in stroke and potential use as biomarkers and therapeutic targets. Aging Dis. *5*, 294–306.

Gao, L., Guan, W., Wang, M., Wang, H., Yu, J., Liu, Q., Qiu, B., Yu, Y., Ping, Y., Bian, X., et al. (2017). Direct generation of human neuronal cells from adult astrocytes by small molecules. Stem Cell Reports *8*, 538–547.

Gouveia, A., Hsu, K., Niibori, Y., Seegobin, M., Cancino, G.I., He, L., Wondisford, F.E., Bennett, S., Lagace, D., Frankland, P.W., and Wang, J. (2016). The aPKC-CBP pathway regulates adult hippocampal neurogenesis in an age-dependent manner. Stem Cell Reports *11*, 719–734.

Jin, K., Sun, Y., Xie, L., Peel, A., Mao, X.O., Batteur, S., and Greenberg, D.A. (2003). Directed migration of neuronal precursors into the ischemic cerebral cortex and striatum. Mol. Cell Neurosci. *24*, 171–189.

Kalluri, H.S., and Dempsey, R.J. (2008). Growth factors, stem cells, and stroke. Neurosurg. Focus *24*, E14.

Karow, M., Sánchez, R., Schichor, C., Masserdotti, G., Ortega, F., Heinrich, C., Gascón, S., Khan, M.A., Lie, D.C., Dellavalle, A., et al. (2012). Reprogramming of pericyte-derived cells of the adult human brain into induced neuronal cells. Cell Stem Cell *11*, 471–476.

Krishnakumar, R., and Blelloch, R.H. (2013). Epigenetics of cellular reprogramming. Curr. Opin. Genet. Dev. *23*, 548–555.

Krueger, H., Koot, J., Hall, R.E., O'Callaghan, C., Bayley, M., and Corbett, D. (2015). Prevalence of individuals experiencing the effects of stroke in Canada: trends and projections. Stroke *46*, 2226–2231.

Li, X., Zuo, X., Jing, J., Ma, Y., Wang, J., Liu, D., Zhu, J., Du, X., Xiong, L., Du, Y., et al. (2015). Small-molecule-driven direct reprogramming of mouse fibroblasts into functional neurons. Cell Stem Cell *17*, 195–203.

Liu, S., Agalliu, D., Yu, C., and Fisher, M. (2012). .The role of pericytes in blood brain barrier function and stroke. Curr. Pharm. Des. *18*, 3653–3662.

Murao, N., Noguchi, H., and Nakashima, K. (2016). Epigenetic regulation of neural stem cell property from embryo to adult. Neuroepigenetics *5*, 1–10.

Nakagomi, T., Kubo, S., Nakano-Doi, A., Sakuma, R., Lu, S., Narita, A., Kawahara, M., Taguchi, A., and Matsuyama, T. (2015). Brain vascular pericytes following ischemia have multipotential stem cell activity to differentiate into neural and vascular lineage cells. Stem Cells *33*, 1962–1974.

Pfisterer, U., Ek, F., Lang, S., Soneji, S., Olsson, R., and Parmar, M. (2016). Small molecules increase direct neural conversion of human fibroblasts. Sci. Rep. *6*, 38290.

Sakuma, R., Kawahara, M., Nakano-Doi, A., Takahashi1, A., Tanaka, Y., Narita, A., Kuwahara-Otani, S., Hayakawa, T., Yagi, H., Matsuyama, T., and Nakagomi, T. (2016). Brain pericytes serve as microglia generating multipotent vascular stem cells following ischemic stroke. J. Neuroinflammation *13*, 57.

Shimada, I.S., LeComte, M.D., Granger, J.C., Quinlan, N.J., and Spees, J.L. (2012). Self-renewal and differentiation of reactive astrocyte-derived neural stem/progenitor cells isolated from the cortical peri-infarct area after stroke. J. Neurosci. *32*, 7926–7940.

Sweeney, M.D., Ayyadurai, S., and Zlokovic, B.V. (2016). Pericytes of the neurovascular unit: key functions and signaling pathways. Nat. Neurosci. *19*, 771–783.

Tatebayashi, K., Tanaka, Y., Nakano-Doi, A., Sakuma, R., Kamachi, S., Shirakawa, M., Uchida, K., Kageyama, H., Takagi, T., Yoshimura, S., et al. (2017). Identification of multipotent stem cells in human brain tissue following stroke. Stem Cells Dev. *26*, 787–797.

Wang, J., Weaver, I.C.G., Gauthier-Fisher, A., Wang, H., He, L., Yeomans, J., Wondisford, F.E., Kaplan, D.R., and Miller, F.D. (2010). CBP histone acetyltransferase activity regulates embryonic neural differentiation in the normal and Rubinstein-Taybi syndrome brain. Dev. Cell *18*, 114–125.

Wang, J., Gallagher, D., DeVito, L., Cancino, I., Tsui, D., He, L., Keller, G., Frankland, P.W., Kaplan, D.R., and Miller, F.D. (2012). Metformin activates atypical PKC-CBP pathway to promote neurogenesis and enhance spatial memory formation. Cell Stem Cell *11*, 23–35.

Stem Cell Reports, Volume *9*

Supplemental Information

The aPKC-CBP Pathway Regulates Post-stroke Neurovascular Remodeling and Functional Recovery

Ayden Gouveia, Matthew Seegobin, Timal S. Kannangara, Ling He, Fredric Wondisford, Cesar H. Comin, Luciano da F. Costa, Jean-Claude Béïque, Diane C. Lagace, Baptiste Lacoste, and Jing Wang

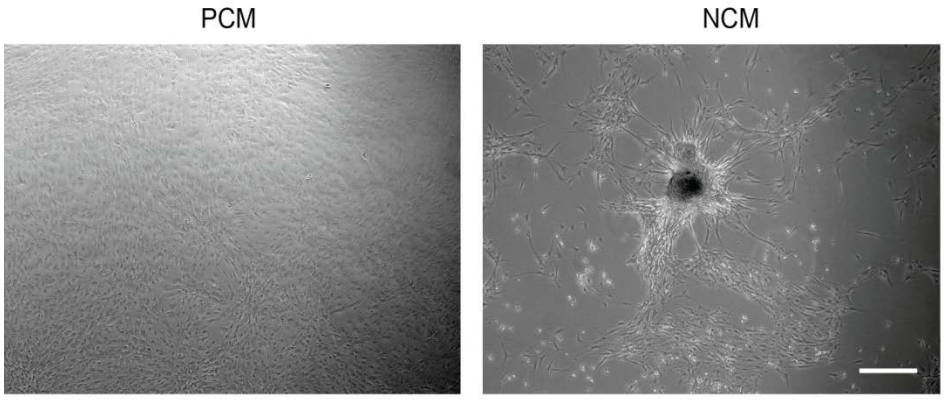

Figure S1. Reprogramming of i-pericytes to neural precursors. Ischemia-activated pericytes were cultured as a monolayer of cells under pericyte conditioned medium (PCM, left panel), while neurospheres were formed in the culture dish when PCM were switched to neural conditioned medium (NCM, right panel). Scale Bar=200μm

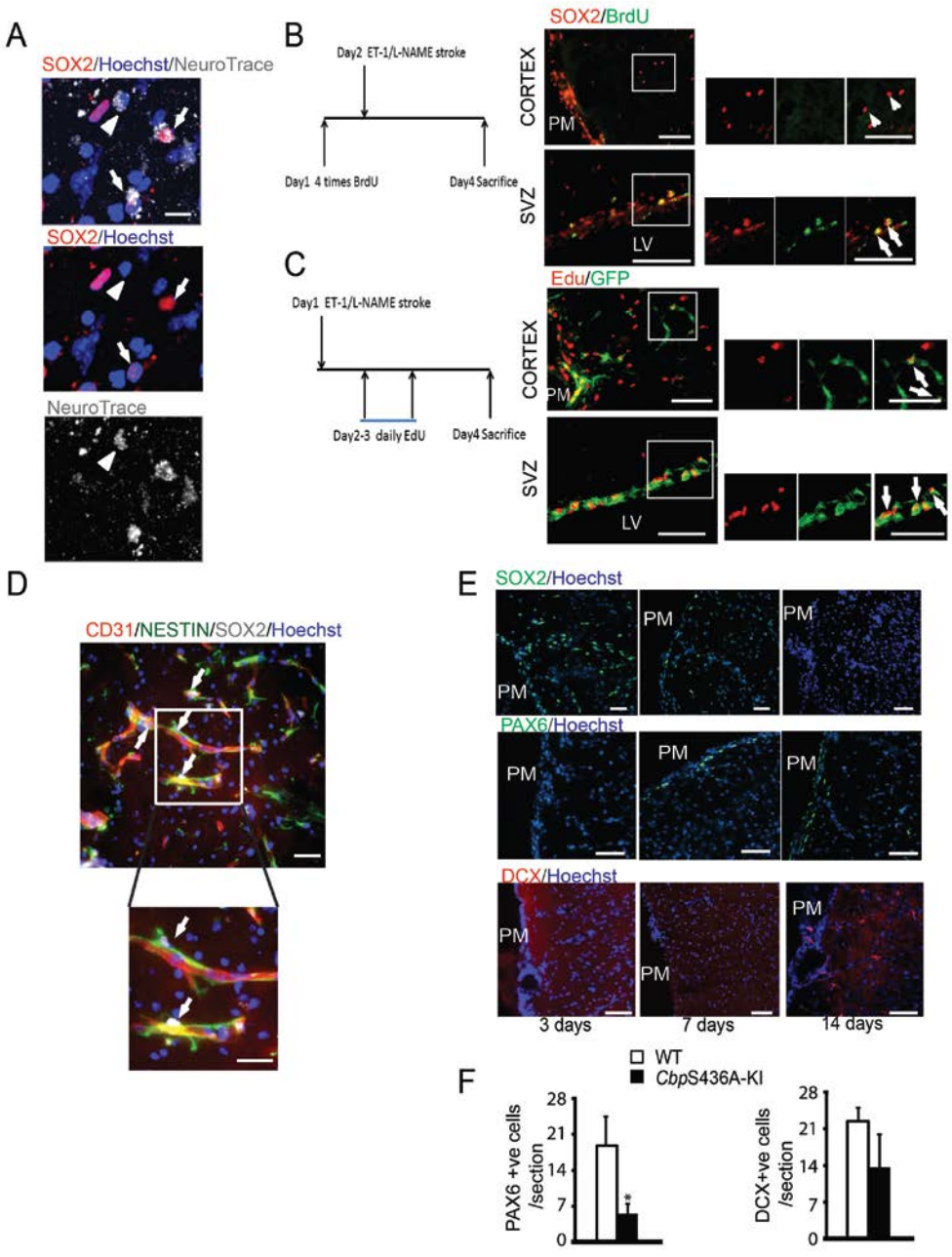

Figure S2. Locally-derived neural precursor cell lineage in cortex layer I following ischemic stroke injury. (A) Merged images from live two-photon imaging for NeuroTrace and confocal imaging for SOX2+NPCs. Scale bar=10μm. (B) Representative micrographs of the ipsilateral cortex and SVZ of mice who received stroke surgery 2 days prior and BrdU (i.p. 60mg/kg, 4

times every 3-hour) injections 24 h pre-surgery, stained for SOX2 (red) and BrdU (green). Arrows denote co-labelled cells, while arrow heads denote single-labeled cells with SOX2+. Scale bar= 40μm; PM: pia mater, LV: lateral ventricle. A flowchart of this experiment is on the left panel. (C) Representative micrographs of the ipsilateral cortex and SVZ of *Sox2-GFP* mice who received stroke surgery 3 days prior and EdU injections (i.p. 50mg/kg, daily) post stroke day 2-3, stained for GFP (green) and EdU (red). Arrows denote co-labelled cells. Scale bar= 40μm. A flowchart of this experiment is on the left panel. (D) Representative micrographs of the ipsilateral cortex 3 days post-stroke show that locally-derived SOX2 (white) + NPCs are adjacent to CD31 (red)+ endothelial cells, colabelled with NESTIN (green). Scale bar=20μm. (E) Representative images of the infarct cortex at days3, 7, 14 post-stroke, stained with SOX2 (green, top), PAX6 (green, middle), and DCX (red, bottom). Scale bar=20μm. (F) Quantitative analysis of PAX6 (left) and DCX (right) positive cells in WT and *Cbp*S436A ipsilateral cortex layer I below the pia surface, 14 days post-stroke, *$p<0.05$, n=3 per group.

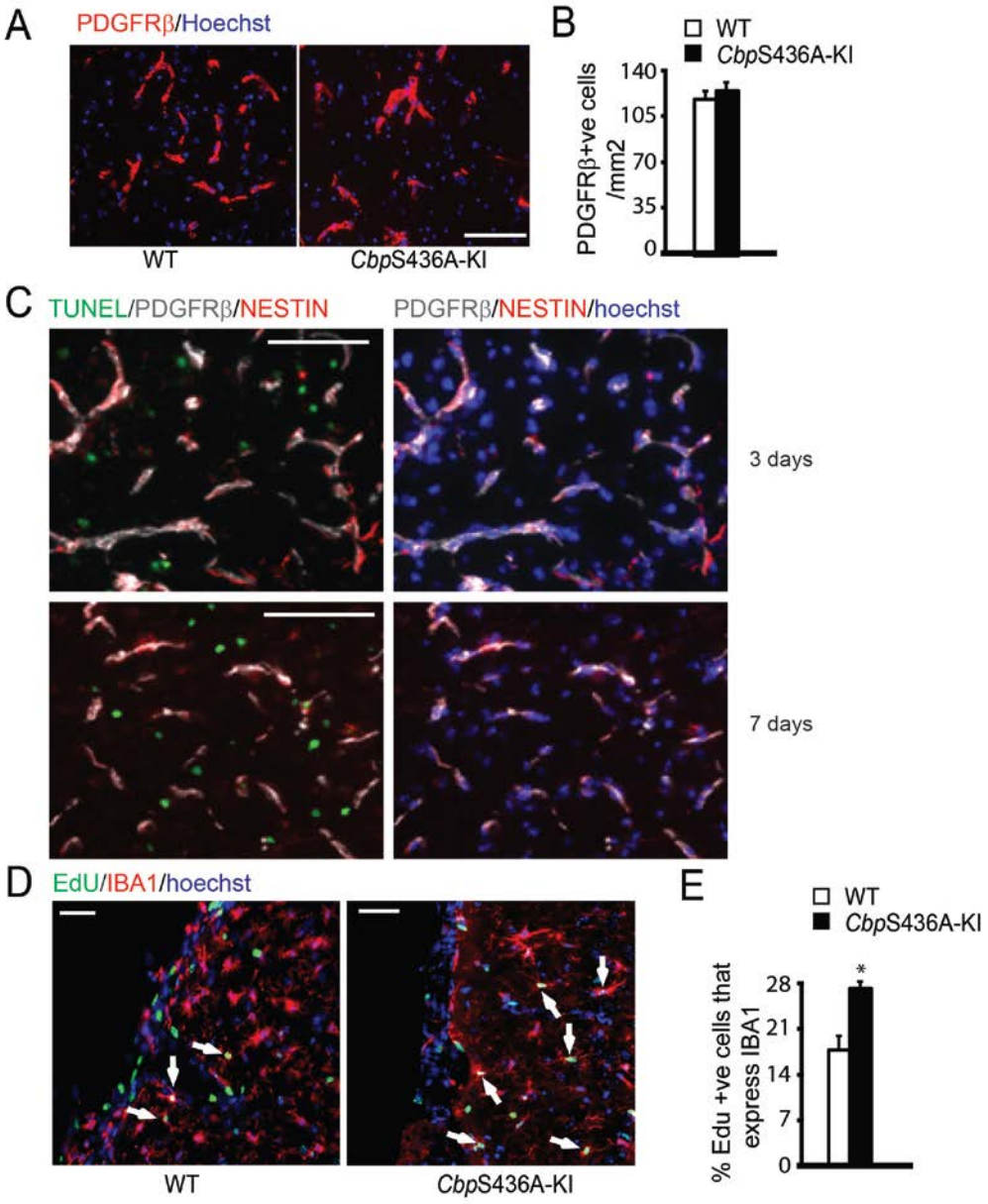

Figure S3. (A-C) Basal number of pericytes and apoptotic i-pericytes remain the same between WT and C*bp*S436A-KI. (A) Representative micrographs of the cortex from both WT and *Cbp*S436A-KI mice under physiological conditions, stained for PDGFRβ (red), counterstained with Hoechst (blue). Scale bar= 40μm (B) Quantitative analysis of PDGFRβ + pericytes in the WT and *Cbp*S436A cerebral cortex as shown in (A) under physiological condtions. n=3/group. (C) Representative micrographs of ipsilateral cortex from WT mice at 3

days and 7 days following stroke surgery, stained for TUNEL (green), PDGFRβ (grey), NESTIN (red), counterstained for Hoechst (blue). Scale bar= 40μm. (D-E) **C*bp*S436A-KI mice show an increase in the population of Iba1+microglia in injured cortex layer I following stroke.** Representative images (D) and quantitative analysis (E) of co-labelled IBA1+/EdU+ cells in WT and *Cbp*S436A ipsilateral cortex 14 days post-stroke, injected with EdU (i.p. 50mg/kg) at post-stroke days 2-5. Scale bar= 25μm. *$p<0.05$, n=3-4/group.

Supplemental Experimental Procedures:

Animals

Only wild type (WT) and homozygous (*Cbp*S436A-KI) mice (Zhou, et al., 2004) were used as experimental mice and heterozygous of *Cbp*S436A were used for breeding. The *Sox2*-GFP reporter transgenic line was provided by Dr. Ruth Slack. The *Nestin*-GFP reporter transgenic line (Yamaguchi, et al., 2000) and *Nestin*Cre-ER^{T2} (Lagace, et al., 2007)/tdTomato$^{flx/Stop/flx}$ transgenic line were provided by Dr. Diane Lagace.

ET-1/L-NAME Surgery

Injections were performed using a Hamilton 10uL gastight syringe with a 0.49mm diameter needle (Hamilton Robotics, Reno NV, 7653-01). Injections of saline, or ET-1 (Abcam, Cambridge, UK, AB120471) (2 µg/ µl) + L-N^{G}-Nitroarginine methyl ester (L-NAME) (Sigma-Aldrich, St. Louis MS, N5751) (2.7 µg/ µl) were performed at +0.0mm anterior-posterior (AP), -2.0mm Medial-Lateral (ML), -1.6mm Dorsal-Ventral (DV); +0.2AP, -2.0ML, -1.4DV; and +0.4AP, -2.0ML, -1.3DV. ET-1 and L-NAME were dissolved in PBS and sonicated in a 4^{o}C water bath for 15 minutes before use. The injection was performed at 0.2 µL/minute for 5 minutes per site for a total of 1µL/injection. Upon needle insertion, 1 minute waiting time was used to allow for settling of tissue. Following injection, a 3-minute waiting time before needle removal was used to reduce back-flow. Body temperatures were continually monitored and maintained at 37^{o}C during surgery using a heating pad and anal thermometer. Local Bupivacaine and subcutaneous buprenorphine were administered post-surgery and 4 hours later. All animals that received strokes were included in the study since Cresyl Violet histological staining (method below) confirmed strokes were produced in all mice and there was no lethality post stroke.

Pericyte Culture and Sphere Formation

The infarct/periinfarct cortical tissue was removed and digested in HBSS for 30 minutes using papain (Worthington Biochemicals, LS003126) and 100 units DNAse (Sigma-Aldrich, D5025-15KU) at 37^{o}C. The samples were then triturated through 18- and 23- gauge needles. Single dissociated cells were plated at 600,000 cells/mL in an uncoated plastic dish with high glucose DMEM/F-12 containing 5µg/mL EGF (VWR, CACB354052), 5µg/mL FGF (Peprotech, 100-18B), 1% N2 supplement (Thermo Fisher, 17502048), and 2% FBS (Life Technologies, 12484010). Full media changes were performed on days 1 and 2 post-plating and half media changes every other day following that.

After 1 week, ischemia-activated pericytes (i-pericyte) were selectively grown, showing 100% population of cells expressing pericyte markers, PDGFRβ and NG2. These i-pericytes were exposed to neural conditioned medium (NCM): DMEM/F-12 media containing 5µg/ml FGF, 5µg/ml EGF, 10µg/mL leukemia inhibitory factor (LIF) (Peprotech, 250-02), and 1% N2 for 2-4 weeks. 100µL of media was added once a week to account for evaporation. After 3 weeks, the total spheres in each well were counted before single spheres were collected onto glass slides using a Cytospin (Thermo Fisher).

Single spheres were also picked and placed into a dish coated with matrigel in neural basal media containing retinoic acid (RA, 200nM) for differentiation. After 1 week cells were stained for βIII TUBULIN, GFAP and O4.

Drug treatment

To label dividing cells, mice received an intraperitoneal injection (i.p.) with 50mg/kg 5 ethynyl 2' deoxyuridine (EdU) (Cedarlane, Burlington, ON, AB16186) prepared in sterile PBS. Injections were given daily for day 2-5 post-stroke for *Cbp*S436A strain, and day 2-3 post-stroke for *Sox2*-GFP mice. A separate cohort of mice received i.p. injections with 60mg/kg 5 bromo2' deoxyuridine (BrdU) (Sigma-Aldrich, B9285) prepared in sterile PBS. Injections were performed beginning 24 hours before surgery and were repeated 4 times, once every 3 hours. To trace SVZ NPCs using *Nestin-CreER^{T2}/tdtomato floxed* transgenic line, tamoxifen (180mg/kg, i.p. daily for 5 days) were injected for 5 days beginning at 12 days before ET-1/L-NAME stroke surgery.

Immunohistochemistry, microscopy, and quantification

At 3 or 14 days post-surgery, mice were anesthetized and transcardially perfused with 4% Paraformaldehyde (PFA) (Sigma-Aldrich, 1518127) in PBS. Then brains were removed and sectioned in a CRYOSTAT (Leica Biosystems, Buffalo Grove IL, CM1850) at 20 μm. Serial sections were mounted on 10 glass slides. Brain sections that were stained for CD31 or PDGFR-β were perfused with PBS, followed by immediate dissection and snap freezing in 100% ethanol cooled with dry ice. The sections were fixed with acetone at room temperature immediately after sectioning. The slides were dried and then were stored at -80^{o}C until needed.

For PFA perfused sections, Two 5-minute washes with PBS were performed before 15-minute fixation with 4^{o}C 4% PFA. For acetone fixed sections; the sections were directly fixed with -20^{o}C acetone for 15 min and dehydrated with -20^{o}C 100% ethanol. Three 5-minute washes

with PBS were performed on all slides sections before proceeding to the permeabilization /blocking step.

Sections were blocked and permeabilized with 10% goat serum (Jackson Immuno-research, West Grove PA, 008-000-121) (horse serum if primary antibody was produced in a goat) and 0.3% Triton-X, and then were incubated with primary antibodies at 4ºC overnight, with secondary antibodies at room temperature for 1 hour, counterstained with Hoechst 33343 (1:2000, Sigma-Aldrich) and mounted using GelTol (Fisher). For BrdU colabelling with SOX2, sections were incubated in 1 N HCl at 60°C for 30 min, rinsed in PBS, incubated in rat anti-BrdU antibody at 4°C overnight, in Alexa 488 donkey anti-rat antibody for 1 hour and then sequentially immunostained for anti-Sox2 followed by Alexa Fluor-conjugated secondary antibodies.

Primary antibodies used were: rat anti-CD31 (1:200) (BD Pharminogen, Franklin Lake, NJ, 550274), rat anti-BrdU (1:200) (AbD Serotec, Oxford UK, OBTOO30G), rabbit anti-SOX2 (1:200) (Millipore, Billiereca MA, 49005), goat anti-DCX (1:200) (Santa Cruz Biotechnologies, Dallas TX, sc-8066), rabbit anti-PDGFR-β (1:100) (Santa Cruz Biotechnologies, sc-1627), Rabbit anti-PAX 6 (1:200)(Biolegend, 901301), chicken anti-NESTIN (1:1000) (Aves labs, NES), Chicken anti-GFP(1:1000)(Abcam, ab13970), rabbit anti-NG2(1:1000)(Milipore, AB5320), rabbit anti-IBA1(1:1000)(Wako Chemicals, 019-19741), rabbit anti-DSRED (1:1000)(Living Colors, 632496), mouse β III TUBULIN (1:1000) (Covance, MMS-435P), rabbit GFAP (1:1000) (Abcam, ab7260), mouse O4 IgM (1:400) (Millipore, MAB345).

Digital image acquisition was performed using either a Zeiss Axioplan 2 fluorescent microscope with Zeiss Axiovision software that contains z-axis capability, or a Zeiss LSM 510 confocal microscope using Zeiss Zen Pro software V2.0 (Oberkochen, Germany). 10-15 images

were captured in the Z-axis per section at a maximum of 1µm apart and processed as an optical stack of 10-15 scanned slices for quantification.

For quantification, positive cells in the desired region were quantified using imageJ software (National Institute of Health, Bethesda MD). Images were obtained at 20x magnification. Three images per section for 6-10 sections were quantified, dependent on the extent of the stroke.

Particle analysis for vascular coverage was performed using ImageJ. The auto threshold function was used in conjunction with particle analysis for area coverage. Particles below 5 pixels were excluded from analysis for area coverage.

Three Dimensional (3-D) Blood Vessel Staining, Imaging and Quantification

The cortices were removed from between the glass and washed with PBS, then embedded in 2% agarose in PBS. The cortices were cut tangentially into 120µm sections using a vibratome (Leica WT1000S). Sections were blocked with 10% horse serum, permeabilized with 0.2% tritonX100 and 0.5% fish gelatin followed by overnight incubation with rat anti-CD31 (BD Pharminogen 550274, 1:200). The sections were then rinsed in PBS and incubated for two hours in anti-rat Alexa fluor 488 conjugated antibodies (Jackson Immunoresearch, 1:300). Slides were mounted with fluoromount G and visualized using fluorescent confocal microscopy (LSM510/Axioimager.M1, Zeiss). Z-Stacks between 60-80µm were obtained.

Two images per hemisphere per section for three sections were analyzed for vessel length and branch points as previously described (Lacoste et al., 2014). Briefly, first, the images were smoothed, followed by application of an adaptive thresholding procedure (Gonzalez & Woods, 2007). The obtained arteries had their medial axes extracted by using a thinning algorithm

(Palàgyi & Kuba, 1998), giving rise to a network (Viana et al., 2009; Rafelski et al., 2012). Bifurcations in such structures were detected as corresponding to pixels with three or more neighbors, while pixels with a single neighbor were understood as terminal nodes. The arc-length of the segments between the bifurcations were then estimated (Cesar Jr. & Costa, 1999). The number of branch points was also obtained.

Two-photon *ex vivo* imaging. Briefly, 3 days following NeuroTrace 500/525 and ET-1/L-NAME injections, mice were deeply anesthetized with isofluorane (Baxter Corporation, Canada), and transcardially perfused with ice-cold, oxygenated choline-based artificial cerebrospinal fluid (choline-aCSF), containing the following (in mM): 119 Choline-Cl, 2.5 KCl, 4.3 $MgSO_4$, 1.0 NaH_2PO_4, 1.0 $CaCl_2$, 11 Glucose, and 26.2 $NaHCO_3$ (pH 7.2-4, 295-310 mOsm/L). Mice were then decapitated and the brain was quickly removed. Coronal slices (300 µm) containing the full extent of the ET-1-induced infarct were generated using a Leica VT1000 S vibratome blade microtome (Leica Microsystems). Brain sections were then transferred to an incubation chamber, and allowed to recover for at least one hour in oxygenated artificial cerebrospinal fluid (aCSF), containing the following (in mM): 119 NaCl, 2.5 KCl, 1.3 $MgSO_4$, 1.0 NaH_2PO_4, 2.5 $CaCl_2$, 11 Glucose, and 26.2 $NaHCO_3$ (pH = 7.2-4, 295-310 mOsm/L) initially maintained at 30^{o}C, then recovered at room temperature. Slices were transferred to a perfusion chamber and immersed in oxygenated aCSF (2 mL/minute) at room temperature. Bright-field imaging of cells within Layer 1-2 of the peri-infarct cortex was conducted using an AxioCam ICm1 CCD camera (Zeiss), coupled to a Zeiss LSM710 multiphoton microscope with a 20x (1.0 NA) objective. Bright-field acquisition allowed the aligning of 2-photon imaging, performed using a Ti:Sapphire pulsed laser tuned to 1000 nm (MaiTai-DeepSee, Spectra Physics), similar to

previously reports *in vivo* (Damisah et al., 2017). Once imaging was complete, slices were post-fixed in 4% paraformaldehyde for 1-3 hours, and then placed in 30% sucrose (in 1x PBS) at 4^{o}C.

Slices were permeabilized in PBS with 0.3% triton for 24 hours at 4^{o}C. The primary antibody against SOX2 was then added for 24 hours at 4^{o}C in 10% normal goat serum. Three PBS washes were performed for 10 minutes and secondary antibody was added overnight at 4^{o}C. The section were mounted and imaged by fluorescent confocal microscopy (LSM510/Axioimager.M1, Zeiss) for the first 30μm of depth. The two-photon and confocal images were compared and landmarked in order to align physical features and cells. Once aligned, the images were merged. All land marking and merging was performed using ImageJ.

TUNEL staining

Mice were sacrificed either 3 or 7 days post-stroke and stained for nicked DNA, a hallmark of apoptosis, using R&D systems Tacs in situ fluorescence TUNEL kit (#4812-60-K). Following TUNEL staining the tissue was stained for NESTIN and PDGFRβ as described above. The ipsilateral cortex was analyzed for the presence of TUNEL^{+}/NESTIN^{+}/PDGFRβ^{+} cells.

Horizontal Ladder Test

Mice were placed at the beginning of a horizontal ladder consisting of two plexiglass walls and irregularly placed metal bars across from their home cage. The home cage was placed at the end of the ladder. The mice were videotaped crossing the bar from slightly below in order to have full view of all four limbs. Five trials per day were videotaped and only trials in which mice made clear, uninterrupted movement across the ladder were later analyzed. The mice were given one day of pre-training and one day of baseline measurements prior to surgery. Mice were re-

tested at 7 and 14 days post-stroke. The videos were later analyzed in a blinded fashion using VLC media player at a reduced speed. Steps in which the mice slipped on or missed a bar, or the use of the wall to support their weight, were counted as an error. The percentage of steps containing an error was reported.

Cylinder Test

Mice were placed in a clear plastic cylinder under red light and were videotaped from above for the time it took for the mice to perform 20 rears. One pre-surgery baseline value was obtained and the mice were re-tested at 7 and 14 days post-stroke. The videos were later analyzed frame-by-frame in VLC media player (Version 2.2.3). The total number of ipsilateral, contralateral, and double paw touches against the cylinder wall was counted. The percentage ipsilateral preference was calculated as:

(total ipsilateral forepaw touches – contralateral forepaw touches) *100) / total forepaw touches

Cresyl Violet Staining and **Infarct Volume Measurement**

Slides containing serially collected sections were dried at 37^{o}C for 15 minutes. The slides were then submerged in cresyl violet solution (Sigma-Aldrich, C5402) (0.2% cresyl violet dissolved in 0.5% acetic acid solution, pH = 3.5) for 20 minutes. Sequential washes in 70%, 95% and 100% ethanol were performed before clearance with citrosolv (Fisher, 22-143-975) clearing agent. The slides were mounted with permount solution and placed on a 37^{o}C slide warmer to dry overnight. Cresyl violet images were captured using an Aperio digital pathology slide scanner (Leica Biosystems) and analyzed using Image J. Infarct volume was calculated based on the previously published paper (Huang, et al., 2013).

Statistical Analysis

Data analysis was performed using GraphPad Prism 6 (Graphpad Software, La Jolla CA). Behavioural analysis was performed using two-way ANOVA with Tukey's post-hoc test. Single comparisons were performed using two-tailed Student's T-test.

References

Cesar, R.M., Jr., and Costa, L.D. (1999). Computer-vision-based extraction of neural dendrograms. J. Neurosci. Methods *93*, 121–131.

Gonzalez, R.C., and Woods, R.E. (2007). Digital Image Processing, Third Edition. (New Jersey: Prentice Hall).

Damisah, E.C., Hill, R.A., Tong, L., Murray, K.N., and Grutzendler, j. (2017) A fluoro-Nissl dye identifies pericytes as distinct vascular mural cells during *in vivo* brain imaging Nature Neurosci *20*, 1023-1032.

Huang, J., Li, Y., Tang, Y., Tang, G., Yang, G.Y., Wang, Y. (2013) CXCR4 antagonist AMD3100 protects blood–brain barrier integrity and reduces inflammatory response after focal ischemia in mice. Stroke *44*, 190-197.

Lacoste, B., Comin, C.H., Ben-Zvi, A., Kaeser, P.S., Xu, X., Costa, L.F., and Gu, C. (2014). Sensory-related neural activity regulates the structure of vascular networks in the cerebral cortex. Neuron *83*, 1117–1130.

Lagace, D.C., Whitman, M.C., Noonan, M.A., Ables1, J.L., DeCarolis, N.A., Arguello, A.A., Donovan, M.H., Fischer, S.J., Farnbauch, L.A., Beech, R.D., DiLeone, R.J., Greer, C.A., Mandyam, C.D. and Eisch, A.J. (2007). Dynamic Contribution of Nestin-Expressing Stem Cells to Adult Neurogenesis. J Neurosci. *27*, 12623–12629.

Lee K.F., Soares C., Thivierge J.P., Beique J.C. (2016). Correlated Synaptic Inputs Drive Dendritic Calcium Amplification and Cooperative Plasticity during Clustered Synapse Development. Neuron *89*,784-799.

Palàgyi, K., and Kuba, A. (1998). A 3D 6-subiteration thinning algorithm forextracting medial lines. Pattern Recognit. Lett. *19*, 613–627.

Rafelski, S.M., Viana, M.P., Zhang, Y., Chan, Y.H., Thorn, K.S., Yam, P., Fung, J.C., Li, H., Costa, Lda.F., and Marshall, W.F. (2012). Mitochondrial network size scaling in budding yeast. Science *338*, 822–824.

Soares C., Lee K.F., Nassrallah W., Beique J.C. (2013). Differential subcellular targeting of glutamate receptor subtypes during homeostatic synaptic plasticity. J Neurosci 33:13547-13559.

Viana, M.P., Tanck, E., Beletti, M.E., and Costa, Lda.F. (2009). Modularity and robustness of bone networks. Mol. Biosyst. *5*, 255–261.

Yamaguchi, M., Saito, H., Suzuki, M., and Mori, K. (2000). Visualization of neurogenesis in the central nervous system using nestin promoter-GFP transgenic mice. Neuroreport. *11*, 1991-6.

Zhou, X.Y., Shibusawa, N., Naik, K., Porras, D., Temple, K., Ou, H., Kaihara, K., Roe, M.W., Brady, M.J., Wondisford, F.E. (2004). Insulin regulation of hepatic gluconeogenesis through phosphorylation of CREB-binding protein. Nat. Med. *10*, 633-637.